J Physiol 587.16 (2009) pp 4091–4104

The Journal of Physiology

Real-time monitoring of cAMP levels in living endothelial cells: thrombin transiently inhibits adenylyl cyclase 6

R.C. Werthmann, K. von Hayn, V.O. Nikolaev, M.J. Lohse and M. Bünemann

Department of Pharmacology and Toxicology, University of Würzburg, Versbacherstrasse 9, 97078 Würzburg, Germany

The crosstalk between Ca^{2+} and cAMP signals plays a significant role for the regulation of the endothelial barrier function. The Ca^{2+}-elevating agent thrombin was demonstrated to increase endothelial permeability and to decrease cAMP levels. Since Ca^{2+} and cAMP signals are highly dynamic, we aimed to study the temporal resolution between thrombin-evoked Ca^{2+} signals and subsequent changes of cAMP levels. Here we conduct the first real-time monitoring of thrombin-mediated regulation of cAMP signals in intact human umbilical vein endothelial cells (HUVECs) by utilising the Ca^{2+}-sensitive dye Fluo-4 and the fluorescence resonance energy transfer (FRET)-based cAMP sensor Epac1-camps. We calibrated *in vitro* FRET responses of Epac1-camps to [cAMP] in order to estimate changes in intracellular [cAMP] evoked by thrombin treatment of HUVECs. After increasing [cAMP] to $1.2 \pm 0.2\ \mu$M by stimulation of HUVECs with isoproterenol (isoprenaline), we observed a transient decrease of cAMP levels by $0.4 \pm 0.1\ \mu$M which reached a minimum value 30 s after thrombin application and 15 s after the thrombin-evoked Ca^{2+} peak. This transient decrease in [cAMP] was Ca^{2+}-dependent and independent of a G_i-mediated inhibition of adenylyl cyclases (ACs). Instead the knock down of the predominant subtype AC6 in HUVECs provided the first direct evidence that the Ca^{2+}-mediated inhibition of AC6 accounts for the thrombin-induced decrease in cAMP levels.

(Received 25 March 2009; accepted after revision 22 June 2009; first published online 22 June 2009)

Corresponding author M. Bünemann: Department of Pharmacology and Toxicology, University of Würzburg, Versbacherstrasse 9, 97078 Würzburg, Germany. Email: m-buenemann@toxi.uni-wuerzburg.de

Abbreviations AC, adenylyl cyclase; CFP, cyan fluorescent protein; Epac, exchange protein directly activated by cAMP; F_{CFP}, CFP fluorescence; F_{YFP}, YFP fluorescence; FRET, fluorescence resonance energy transfer; GAPDH, glyceraldehyde-3-phosphate dehydrogenase; HUVEC, human umbilical vein endothelial cell; 8MM-IBMX, 8-methoxymethyl-isobutylmethylxanthine; PAEC, pulmonary artery endothelial cell; PAR-1, protease-activated receptor 1; PDE, phosphodiesterase; PMVEC, pulmonary microvascular endothelial cell; PTX, pertussis toxin; *R*, ratio; siRNA, small interfering RNA; YFP, yellow fluorescent protein.

Endothelial cells provide a semi-permeable barrier between blood and interstitial tissues. The barrier function of endothelial cells is established by close cell–cell tethering mediated by adherens and tight junctions and by adhesion of the cells to the extracellular matrix. Maintenance or disruption of this barrier is regulated by different pathways, many of them converging on regulation of intracellular Ca^{2+} and cAMP signals (Michel & Curry, 1999; Mehta & Malik, 2006).

Thrombin and inflammatory agonists enhance endothelial permeability by triggering a rise in $[Ca^{2+}]_i$ (Lum *et al.* 1989). Upon stimulation of the protease-activated receptor 1 (PAR-1) with thrombin, activation of the G_q signalling cascade results in release of Ca^{2+} from the endoplasmic reticulum (Barr *et al.* 1997; Bogatcheva *et al.* 2002). As a consequence, store- and receptor-operated Ca^{2+} channels in the plasma membrane are activated, leading to Ca^{2+} influx from the extracellular space also termed capacitative Ca^{2+} entry (Putney & Bird, 1993). Physiologically, the increase in $[Ca^{2+}]_i$ precedes endothelial cell contraction and disassembly of inter-endothelial junctions leading to an increased endothelial permeability (Wysolmerski & Lagunoff, 1990; Garcia *et al.* 1995; Bogatcheva *et al.* 2002; Vandenbroucke *et al.* 2008).

However, there is some evidence that the increase in $[Ca^{2+}]_i$ only enhances endothelial permeability if cAMP levels are low (Carson *et al.* 1989; Minnear *et al.* 1989; Cioffi *et al.* 2002). A local rise of [cAMP] at the cell membrane prevents thrombin-induced cell gap formation by increased adhesion of adjacent endothelial cells and of endothelial cells to the extracellular matrix (Garcia *et al.* 1995; Carson *et al.* 1989; Minnear *et al.* 1989; Stelzner *et al.* 1989). On the other hand, a cytosolic cAMP pool generated by soluble adenylyl cyclases (AC) was suggested to support endothelial cell gap formation and this effect even dominated over the barrier protective

DOI: 10.1113/jphysiol.2009.172957

effects of cell membrane-located cAMP pools (Sayner *et al.* 2006).

cAMP and Ca^{2+} signals are not entirely independent, but rather are subject to crosstalk; this interplay can either be mediated by Ca^{2+}-regulated ACs (Willoughby & Cooper, 2007; Sadana & Dessauer, 2009) or Ca^{2+}–calmodulin-dependent phosphodiesterase 1 (PDE1; Goraya & Cooper, 2005).

Endothelial cells express the Ca^{2+}-inhibited subtypes AC5 and AC6 (Manolopoulos *et al.* 1995; Stevens *et al.* 1995; Chetham *et al.* 1997; Bundey & Insel, 2003) and it was suggested that their direct Ca^{2+}-mediated inhibition (Mou *et al.* 2009) may contribute to endothelial cell gap formation in inflammation (Stevens *et al.* 1995; Cioffi *et al.* 2002). Stimulation of endothelial cells with agonists that increase $[Ca^{2+}]_i$ was demonstrated to decrease basal and elevated cAMP levels up to 50%. So far, a Ca^{2+}-induced decrease in [cAMP] in endothelial cells has been detected by means of radioimmuno-based assays and, therefore, changes in [cAMP] were detected after incubating cells with Ca^{2+}-elevating agents such as thrombin for prolonged times ($\geq$5 min) (Stevens *et al.* 1999; Cioffi *et al.* 2002; Creighton *et al.* 2003). However, thrombin-induced Ca^{2+} and cAMP signals can be very rapid and exhibit complex temporal patterns. Therefore, we studied thrombin-induced cAMP regulation with high temporal resolution.

Using the fluorescence resonance energy transfer (FRET)-based cAMP sensor Epac1-camps (Nikolaev *et al.* 2004), changes in [cAMP] can be monitored in real time in single living cells. Thus, we examined the temporal pattern of thrombin-induced Ca^{2+} and cAMP signals by accomplishing the first real-time monitoring of cAMP signals in Epac1-camps-transfected human umbilical vein endothelial cells (HUVECs). More precisely, we studied the impact of a thrombin-mediated increase in $[Ca^{2+}]_i$ on elevated cAMP levels of isoproterenol-prestimulated HUVECs. Thereby we observed a transient thrombin-mediated decrease of cAMP levels and calculated the changes in [cAMP] according to an *in vitro* calibration of FRET changes of Epac1-camps to [cAMP]. By a small interfering RNA (siRNA)-mediated downregulation of AC6 in HUVECs, we provide the first direct evidence that a thrombin-induced decrease in [cAMP] is due to the direct Ca^{2+}-mediated inhibition of adenylyl cyclases.

Methods

Cell culture and cell transfection

Human umbilical vein endothelial cells (HUVECs; Lonza, Cologne, Germany) were cultured in complete medium (EBM-2; Lonza) and grown in the presence of 5% CO_2 at 37°C. HUVECs were transfected with plasmid DNA using Amaxa Nucleofector Technology according to the manufacturer's instructions (Basic Nucleofector Kit for Primary Endothelial Cells; Lonza). HUVECs (5×10^5) were transfected with a maximum of 3 μg DNA. Transfection of HUVECs with the plasmid encoding Epac1-camps (Nikolaev *et al.* 2004) via electroporation yielded transfection efficiencies of over 50%. For FRET measurements, HUVECs were seeded on fibronectin-coated glass coverslips (Human Plasma Fibronectin Purified Protein; Millipore, Schwalbach, Germany) and FRET experiments were done 24 h after transfection.

Non-targeting siRNA, human AC5 siRNA and human AC6 siRNA were purchased from Dharmacon (Thermo Fisher Scientific, Bonn, Germany) as a pool of four independent siRNAs, respectively (siGENOME SMARTpool). Transfection of siRNA was performed 72 h before FRET experiments using Lipofectamine 2000 (Invitrogen, Eugene, OR, USA) according to the manufacturer's instructions. HUVECs at 70% confluency in a 5 cm dish were transfected with a total amount of 600 pmol siRNA (non-targeting siRNA or a mixture of AC5 and AC6 siRNA). After 6 h the medium was replaced and 2 days after siRNA transfection, cells were transfected with Epac1-camps (Nikolaev *et al.* 2004) for FRET measurements. Detection of VE-cadherin distribution with a human VE-cadherin antibody in double-transfected HUVECs indicated that endothelial cells still form monolayers and exhibit typical cell–cell junctions similar to non-transfected cells (see online Supplemental Fig. 1). For detection of VE-cadherin distribution, confluent HUVECs on glass coverslips were fixed for 10 min with 2% paraformaldehyde. Then, monolayers were treated with 0.1% Triton X-100 for 5 min. After rinsing the cells, monolayers were preincubated for 30 min with 10% normal donkey serum and incubated overnight at 4°C with human VE-cadherin antibody (1 : 100, Santa Cruz, Heidelberg, Germany). After several rinses, monolayers were incubated for 60 min with Cy3-labelled donkey anti-goat IgG (1 : 600).

HEK-tsA 201 cells were cultured in Dulbecco's modified Eagle's medium (PAN-biotech, Aidenbach, Germany) supplemented with 2 mM glutamine, 10% fetal calf serum, 0.1 mg ml^{-1} streptomycin and 100 U ml^{-1} penicillin in an atmosphere of 5% CO_2. HEK-tsA 201 cells were transfected with a mixture consisting of DNA (2 μg), DMEM and 12.5 μg polyethyleneimine (Sigma-Aldrich, St Louis, MO, USA) in a total volume of 625 μl. The mixture was incubated for 30 min and then put onto the cells in a 5 cm dish.

Reagents

Adenosine desaminase (0.5 U ml^{-1}; Roche, Palo Alto, CA, USA) was added to the medium 30 min before

each FRET experiment. For testing G_i-mediated effects, cells were incubated with 0.2 mg ml^{-1} pertussis toxin (PTX; Sigma-Aldrich) for 6 h before FRET measurements. The PDE1 selective inhibitor 8-methoxymethyl-isobutylmethylxanthine (8MM-IBMX) was added to the medium at least 30 min before experiments and was present in the buffer during FRET experiments (50 μM; Sigma-Aldrich). Isoproterenol (Sigma-Aldrich) was utilized at 10 nM or 1 μM, and forskolin (Tocris, Bristol, UK) was used at 3 μM to increase cAMP levels in FRET measurements. Thrombin from human plasma (Sigma-Aldrich) was used at 10 U ml^{-1}. The calcium ionophor A23187 (Sigma-Aldrich) was added at 1 μM to increase intracellular Ca^{2+}. For the *in vitro* calibration of Epac1-camps we used cAMP from Sigma-Aldrich.

FRET measurements

Fluorescence microscopy and FRET measurements were done as described previously (Hein *et al.* 2006). Confluent HUVECs that were transfected with Epac1-camps and grown on fibronectin-coated glass coverslips, were placed on an Axiovert 200 inverted microscope (Zeiss, Jena, Germany) using a 63× oil immersion objective, a dual-emission photometric system and a xenon camp based polychrome IV light source (both TILL Photonics, Gräfelfing, Germany). Illumination time was 50 ms at a frequency of 1 Hz. Excitation wavelength was set to 436 ± 10 nm (beam splitter DCLP 460 nm), and emission of single whole cells was recorded at 535 ± 15 and 480 ± 20 nm (beam splitter DCLP 505 nm). The FRET-based sensor Epac1-camps consists of a single cAMP-binding domain derived from exchange protein directly activated by cAMP 1 (Epac1), which is flanked by a yellow fluorescent protein (YFP) and a cyan fluorescent protein (CFP) on either side. In the absence of cAMP this sensor exhibits strong FRET. If cAMP is bound to the binding domain, FRET is highly attenuated (Nikolaev *et al.* 2004). Upon excitation of CFP in intact single cells, CFP and YFP fluorescence intensities and ratiometric FRET signals were recorded as a read-out for cAMP concentrations. Ratiometric FRET signal (R) was calculated as the ratio of yellow fluorescent protein emission (F_{YFP}) over cyan fluorescent protein emission (F_{CFP}), where F_{YFP} was the emission at 535 nm, corrected for direct excitation of YFP at 436 nm and bleedthrough of CFP emission into the YFP channel. Additionally, ratiometric FRET signals of all experiments were normalised to the FRET ratio at the timepoint 0 s (R_0). Cells were continuously superfused with external buffer (mM: NaCl 141, KCl 5.4, MgCl 1, Hepes 10 at pH 7.3) with or without Ca^{2+} (2 mM $CaCl_2$ or 5 mM EGTA). These reagents were from AppliChem (Darmstadt, Germany). Agonists (isoproterenol, thrombin) were freshly prepared and applied using a rapid superfusion system (ALA Scientific Instruments, Westbury, NY, USA).

In vitro calibration of Epac1-camps

HEK-tsA 201 cells, 40 h after transfection with Epac1-camps, were washed three times with phosphate-buffered saline and resuspended in 5 mM Tris-HCl and 2 mM EDTA (pH = 7.4). After disruption of the cells using an Ultra Turrax device for 20 s on ice and 20 min centrifugation at 278 835 g, fluorescence emission spectra of the supernatant (excitation at 436 nm, emission range 460–550 nm) were measured using a fluorescence spectrometer LS50B (PerkinElmer Life Sciences, Waltham, MA, USA) before and after adding various concentrations of cAMP (Sigma-Aldrich) (Nikolaev *et al.* 2004). Peak maxima of CFP (F_{CFP}) and YFP fluorescence (F_{YFP}) were determined. F_{YFP}/F_{CFP} and $\Delta F_{YFP}/F_{CFP}$ (relative to basal F_{YFP}/F_{CFP} without cAMP binding) were calculated and [cAMP] was plotted against $\Delta F_{YFP}/F_{CFP}$ as a per cent of maximal $\Delta F_{YFP}/F_{CFP}$ using Prism 4.0 software (San Diego, CA, USA).

Ca^{2+} measurements

Changes in cytosolic Ca^{2+} levels were monitored in HUVECs loaded with the fluorescent Ca^{2+}-sensitive dye Fluo-4 AM (Molecular Probes, Invitrogen). HUVECs were incubated with 2 μM Fluo-4 AM for 20 min at 37°C and washed with external buffer before fluorescence measurements. Fluo-4 fluorescence was recorded with the same photometric microscope set-up as described for FRET measurements. Illumination time was 50 ms at a frequency of 1 Hz. Excitation wavelength was set to 490 nm (exciter ET470/40×, dichroic T495LP), and emission of single whole cells was recorded at 535 ± 15 nm (DCLP 505 nm). The fluorescence intensity of Fluo-4 increases upon Ca^{2+} binding.

RNA isolation and real-time quantitative PCR

Total RNA was prepared from HUVECs that were transfected with either a non-targeting siRNA pool or AC5/6 siRNA pools, with peqGOLD TriFast (peQLab, Erlangen, Germany) according to the manufacturer's instructions. cDNA was synthesised using SuperScript II reverse transcriptase (Invitrogen) and oligo-dT primers. Real-time PCR was performed using iQ SYBR Green Supermix, iCycler and iCycler iQ real-time detection software for determination of threshold cycle values (Bio-Rad, Hercules, CA, USA). Transcripts of AC5 and AC6 were amplified using primer sequences that are specific for human AC5 and AC6, respectively (AC5: forward 5′-GCACAGGAGCACAACATCAG-3′, reverse 5′-CTCATCTACGTGCTCATCGTG-3′; AC6: forward

5′-CAAACAATGAGGGTGTCGAGT-3′, reverse 5′-TGCTACCAATCGTCTTGATCTT-3′). Glyceraldehyde-3-phosphate dehydrogenase (GAPDH) transcripts were used as a reference (forward 5′-CCAGGCGCCCAATACG-3′, reverse 5′-CCACATCGCTCAGACACCAT-3′). PCR conditions were as follows: 2 min initial cycle at 94°C, 40 cycles of 94°C for 15 s, 56°C for 30 s and 72°C for 40 s.

Using the $2^{-\Delta\Delta CT}$ method (Livak & Schmittgen, 2001), the fold change in AC5 and AC6 gene expression normalised to GAPDH gene expression was calculated relative to control cells.

Western blot analysis

To prove the efficient inhibition of G_i protein via PTX (Sigma-Aldrich) Western blot analysis of phosphorylated ERK (p-ERK) was performed. HUVECs grown in a 12-well plate were kept in media without serum and supplements for 6 h with or without PTX (0.2 mg ml^{-1}). Then cells were collected in 0.3 ml lysis buffer (Roti-load, Roth, Karlsruhe, Germany, containing 50 mM NaF, 5 mM $Na_4P_2O_7$, 0.1 mM Na_3VO_4, 1 mM PMSF, 0.06 mg ml^{-1} benzamidin). Equal amounts of protein were separated by 10% SDS-polyacrylamide gel electrophoresis and then transferred to Immobilon-P membranes (Millipore, Schwalbach, Germany). Membranes were incubated for 1 h in blocking buffer (10 mM Tris-HCl, pH 7.5, 150 mM NaCl, 5% non-fat dry milk, 0.1% Tween-20; AppliChem, Darmstadt, Germany) and then incubated overnight at 4°C with polyclonal rabbit p-ERK antibody (1 : 1000; Cell Signaling, Danvers, MA, USA) in washing buffer (50 mM Tris-HCl, pH 7.5, 150 mM NaCl, 0.2% BSA, 0.2% NP-40; AppliChem, Darmstadt, Germany). After rinsing three times with washing buffer, membranes were incubated with IgG–horseradish peroxidase-conjugated secondary antibody (1 : 10000). After washing three times with washing buffer, signals were visualised by chemiluminescent detection (Amersham ECL Plus; GE Healthcare, München, Germany). To confirm the loading of equal amounts of protein, membranes were incubated in stripping buffer (100 mM glycin, 0.1% SDS, HCl, pH 2.5; AppliChem), before incubation with blocking buffer, polyclonal rabbit ERK antibody (1 : 1000; Cell Signaling) and peroxidase-conjugated secondary antibody (1 : 10 000).

Data analysis and statistics

Fluorescence intensities were acquired using CLAMPEX 9.0 (Axon Instruments, Foster City, CA, USA). Data were processed using Origin 6.1 (Northampton, MA, USA) and statistical analyses were performed using Prism 4.0. Values are given as mean ± S.E.M. For comparison of two individual groups, Student's unpaired *t* tests were performed and differences were considered significant when $P < 0.01$ (two-tailed).

Results

Stimulation of HUVECs with Ca^{2+}-increasing agents induces a transient decrease of elevated cAMP levels

A fine-tuned regulation of Ca^{2+} and cAMP signals is highly relevant for the maintenance or disruption of the endothelial barrier. Therefore, we studied the relationship between the two signals and were especially interested in the temporal pattern of thrombin-induced Ca^{2+} and cAMP signals. To address this question in real time in living cells, we utilised the Ca^{2+}-sensitive dye Fluo-4 and the FRET-based cAMP sensor Epac1-camps (see Methods; Nikolaev *et al.* 2004).

As Ca^{2+}-elevating agonists like thrombin were reported to increase endothelial permeability only if cAMP levels are low (Carson *et al.* 1989; Minnear *et al.* 1989; Cioffi *et al.* 2002) we were especially interested to see if Ca^{2+} signals are capable of lowering elevated cAMP levels that would permit a consequent increase in endothelial permeability. Therefore, we prestimulated HUVECs with the β-adrenergic agonist isoproterenol or directly activated ACs using forskolin in all experiments. First, we tested the effect of the Ca^{2+} ionophore A23187 (1 μM) on cAMP levels after activation of ACs with 3 μM forskolin (Fig. 1*A*). Incubation of cells with 3 μM forskolin led to a decrease in F_{YFP} and an increase in F_{CFP}, resulting in a decrease of the ratiometric FRET signal (R/R_0), which is consistent with an increase in [cAMP]. After reaching a steady-state FRET signal, the addition of 1 μM A23187 resulted in a transient increase of the ratiometric FRET signal, indicative of a transient decrease in [cAMP] (Fig. 1*A*).

We next probed the impact of thrombin on pre-elevated cAMP levels. To investigate the relationship of the kinetics of Ca^{2+} and cAMP signals in HUVECs. we also studied thrombin-induced Ca^{2+} signals in Fluo-4-labelled HUVECs (Fig. 1*B*). The averaged Fluo-4 intensities (mean ± S.E.M., $n = 13$, Fig. 1*B*) demonstrated that the Ca^{2+} signals peaked approximately 15 s after thrombin application. Figure 1*C* illustrates a thrombin-induced (10 U ml^{-1}) transient increase of ratiometric FRET signals (R/R_0) in HUVECs that were prestimulated with 10 nM isoproterenol, indicative of a transient decrease in [cAMP]. The transient ratiometric FRET signal peaked about 30 s after thrombin treatment (mean ± S.E.M., $n = 14$). These results demonstrated that thrombin application led to a transient increase in [Ca^{2+}] and a subsequent transient decrease in pre-elevated [cAMP]. If HUVECs were not prestimulated with forskolin or isoproterenol to elevate cAMP levels, the thrombin-mediated decrease in [cAMP] could not be observed as further reduced cAMP levels are below the

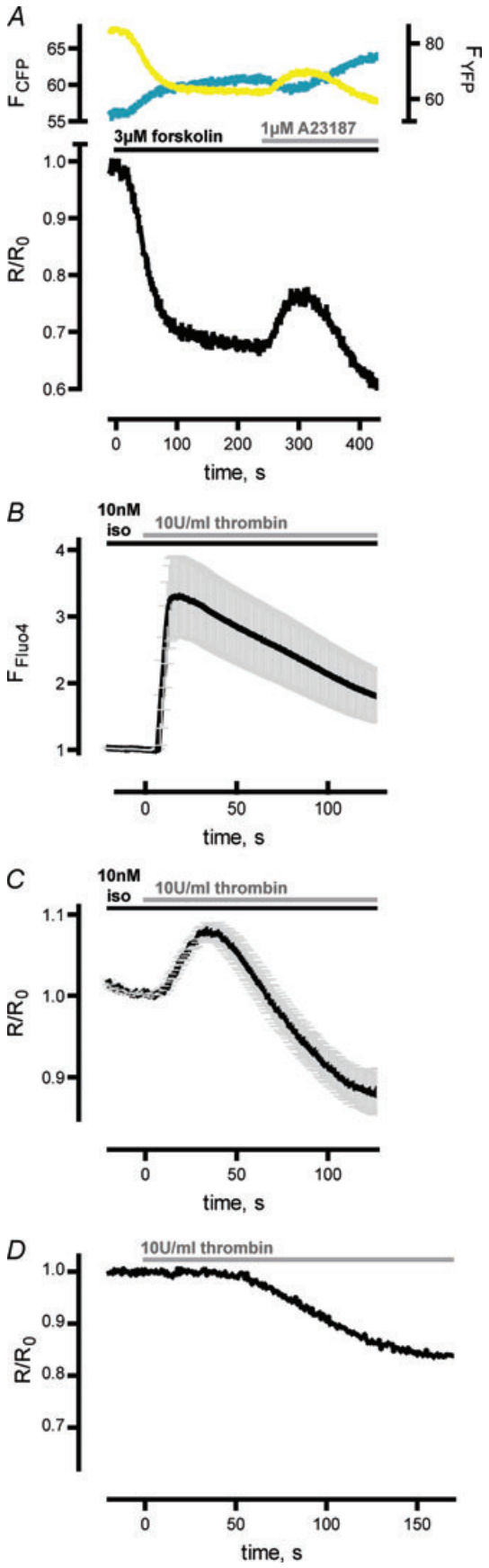

detection limit of Epac1-camps; however, we surprisingly detected a delayed thrombin-mediated increase in [cAMP] (Fig. 1*D*). The mechanism leading to an increase of cAMP levels is the topic of ongoing studies.

Decrease of cAMP levels is Ca^{2+} dependent and $G_{i/o}$ independent

The thrombin-induced decrease of cAMP levels could be potentially caused by either G_i protein-mediated inhibition of ACs, Ca^{2+}-mediated activation of phosphodiesterase 1 (PDE1), or Ca^{2+}-mediated inhibition of AC5 and AC6. The thrombin receptor PAR-1 was shown to activate G_i proteins in rat adrenal medullary microvascular endothelial cells and in these cells a thrombin-induced decrease in [cAMP] was related to G_i-mediated inhibition of adenylyl cyclases (Manolopoulos *et al.* 1997). To check the involvement of G_i protein activation, we incubated HUVECs with the G_i protein inhibitor PTX (0.2 mg ml^{-1}) for more than 6 h. However, the thrombin-mediated increase in FRET was still detectable as shown in a representative experiment in Fig. 2*A*. In order to quantify thrombin-induced alterations in [cAMP], we defined thrombin-induced changes of ratiometric FRET signals as $R_{\text{thrombin}} - R_{\text{iso}}$ (Fig. 2*A*), where R_{iso} defines the decreased ratiometric FRET signals after stimulation of cells with isoproterenol and R_{thrombin} marks the ratiometric FRET signal 30 s after addition of thrombin (mean time delay until reaching the maximum

Figure 1. Stimulation of HUVECs with Ca^{2+}-increasing agents led to a transient decrease of pre-elevated cAMP levels
A, upon CFP excitation, YFP and CFP fluorescence was recorded in single HUVECs expressing the FRET-based cAMP sensor Epac1-camps. Activation of adenlylyl cyclases with 3 μM forskolin led to a decrease in YFP emission (F_{YFP}, yellow trace, corrected for direct excitation and bleed through) and a concomitant increase in CFP emission (F_{CFP}, cyan trace). The ratiometric FRET signal was normalised to R_0 (R/R_0, lower panel) which is the FRET ratio at timepoint 0 s. The decrease in FRET is consistent with an increase in [cAMP]. Addition of the Ca^{2+} ionophor A23187 (1 μM) led to a transient increase in FRET representing a transient decrease in [cAMP] (representative experiment shown). *B*, Fluo-4-loaded HUVECs were first stimulated with 10 nM isoproterenol (iso) before addition of thrombin (10 U ml^{-1}). Upon thrombin application, Ca^{2+} binding to Fluo-4 led to a transient increase in the emission intensity induced by excitation with 490 nm. The fluorescence intensity of single experiments was normalised for detection of mean ± S.E.M. ($n = 13$). The averaged Ca^{2+} signal peaked about 15 s after thrombin application. *C*, FRET measurements with Epac1-camps-transfected HUVECs revealed a transient increase in FRET after addition of thrombin (10 U ml^{-1}) to cells prestimulated with 10 nM isoproterenol. The mean ± S.E.M. of normalised ratiometric FRET signals (R/R_0) was calculated ($n = 14$). The averaged transient FRET signal reached a peak approximately 30 s after addition of thrombin. *D*, thrombin (10 U ml^{-1}) led to a delayed decrease in FRET, when HUVECs were not prestimulated with forskolin or isoproterenol (representative experiment shown). There was no transient increase in FRET (compare *A* and *C*).

increase of ratiometric FRET signals, Fig. 1*C*). Statistical analysis of FRET experiments ($n = 10$) revealed no difference in $R_{\text{thrombin}} - R_{\text{iso}}$ of PTX-treated cells (0.058 ± 0.010, mean ± S.E.M.) compared to control cells (0.057 ± 0.008, Fig. 2*B*). Thus, we concluded that the thrombin-mediated increase in FRET was not due to a G_i-mediated inhibition of ACs. The basal FRET ratio (R_0) before isoproterenol stimulation was not significantly different in PTX-treated cells (1.63 ± 0.10) *versus* control cells (1.58 ± 0.08), so we concluded that basal cAMP levels were similar. There was also no significant difference in the initial FRET change after isoproterenol prestimulation of HUVECs ($R_{\text{iso}} - R_0$) after PTX treatment (-0.259 ± 0.030, $n = 10$) compared to control cells (-0.266 ± 0.040, $n = 10$, data not shown). To confirm an effective inhibition of G_i proteins by PTX, we performed p-ERK Western blot assays. Phosphorylation of ERK was reduced in PTX-treated HUVECs compared to control cells ($26.7 \pm 5.4\%$; $n = 3$; Supplemental Fig. 2).

To confirm a Ca^{2+}-mediated effect, we repeated experiments with PTX-treated HUVECs using EGTA-buffered external solution without Ca^{2+} to prevent capacitative Ca^{2+} entry. This led to a significant reduction ($P < 0.01$) of the thrombin-mediated increase in FRET ($R_{\text{thrombin}} - R_{\text{iso}}$, Fig. 2*B*) compared to PTX-treated control cells. Thus, the thrombin-induced increase in FRET is Ca^{2+}-dependent. To test whether a Ca^{2+}-mediated activation of the Ca^{2+}-regulated PDE1 caused hydrolysis of cAMP, we next incubated HUVECs with the selective PDE1 inhibitor 8MM-IBMX and added the Ca^{2+} ionophore A23187 after prestimulation with 3 μM forskolin (compare Fig. 1*A*). However, FRET experiments revealed no significant difference in $R_{\text{A23187}} - R_{\text{forskolin}}$, whether cells were 8MM-IBMX treated (0.056 ± 0.012, mean ± S.E.M., $n = 8$) or not ($0.080 \pm 0.010\%$, $n = 10$; data not shown). Preincubation of HUVECs with 8MM-IBMX did also not significantly alter basal FRET ratio (1.69 ± 0.14) compared to control cells (1.63 ± 0.15), and the forskolin-induced FRET change ($R_{\text{forskolin}} - R_0$) was also not significantly different in cells treated ($-0.342 \pm 0.020\%$, mean ± S.E.M., $n = 8$) or non-treated (-0.306 ± 0.017, $n = 10$) with 8MM-IBMX. The functionality of the PDE1 inhibitor was controlled for by using PDE1-expressing cells (primary smooth muscle cells). The acute addition of 8MM-IBMX to these cells caused a decrease in FRET (data not shown), consistent with an increase in [cAMP], which confirms the functionality of 8MM-IBMX. Therefore, we exclude a major contribution of the Ca^{2+}-regulated PDE1 to the observed increase in FRET in HUVECs.

Transient change in [cAMP] may be caused by Ca^{2+}-mediated regulation of adenylyl cyclases

Adenylyl cyclases can either be activated (AC1, AC8) or inhibited (AC5, AC6) by an increase in intracellular [Ca^{2+}]. If the thrombin-induced increase in FRET is caused by a Ca^{2+}-mediated regulation of ACs, overexpression of Ca^{2+}-regulated or Ca^{2+}-independent ACs should affect $R_{\text{thrombin}} - R_{\text{iso}}$. Therefore, HUVECs were transfected with plasmids encoding Ca^{2+}-inhibited

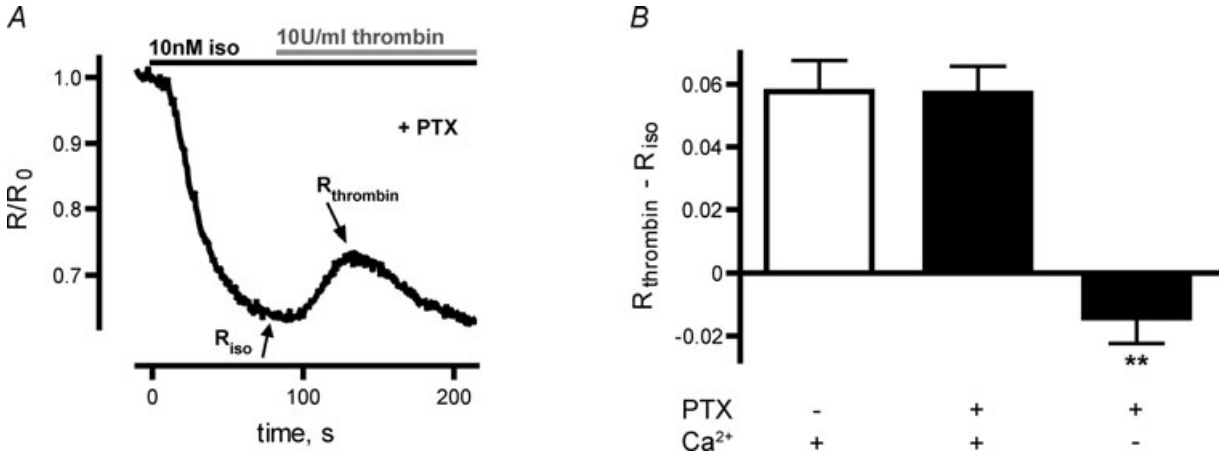

Figure 2. Thrombin-induced decrease of cAMP levels was insensitive to PTX and dependent on elevation of $[Ca^{2+}]_i$

A, a representative FRET experiment shows a thrombin-mediated increase in FRET despite PTX treatment to prevent G_i activation. R_{iso} and R_{thrombin} mark the minimal FRET ratio after isoproterenol stimulation and the FRET ratio about 30 s after thrombin application, respectively. *B*, the thrombin-induced increase of the ratiometric FRET signal, defined by $R_{\text{thrombin}} - R_{\text{iso}}$, of PTX-incubated cells was similar to that under control conditions ($n = 9$). However, $R_{\text{thrombin}} - R_{\text{iso}}$ was reduced in PTX-treated HUVECs, that were measured in EGTA-buffered external solution without Ca^{2+} (**$P < 0.01$).

AC6 and Ca^{2+}-independent AC4, respectively. Figure 3*A* shows a representative FRET trace of HUVECs transfected with AC6. Overexpression of AC6 resulted in a slightly increased isoprenaline-induced decrease in FRET (Fig. 3*C*) and a significantly enhanced thrombin-induced increase in FRET compared to control cells ($P < 0.01$, Fig. 3*D*). However, overexpression of AC4 surprisingly led to a thrombin-mediated decrease in FRET as depicted in a representative FRET experiment (Fig. 3*B*), potentially uncovering an opposing pathway leading to a thrombin-induced elevation of cAMP levels. Overexpression of AC4 also resulted in a significant repression of the isoprenaline-induced decrease of ratiometric FRET signals ($R_{iso} - R_0$, $P < 0.01$, Fig. 3*C*). In fact, examination of $R_{thrombin}$ values 30 s after thrombin application revealed negative values of $R_{thrombin} - R_{iso}$ (Fig. 3*D*) because of the thrombin-induced decrease in FRET.

The monomolecular cAMP sensor Epac1-camps allows the determination of [cAMP] based on ratiometric FRET signals. Therefore, we performed an *in vitro* calibration of Epac1-camps based on [cAMP] (Fig. 3*E*). The established *in vitro* concentration–response curve yielded an EC_{50} value of 1.5 μM cAMP (compare Nikolaev *et al.* 2004). To translate this *in vitro* calibration into reliable estimates of [cAMP] in intact cells based on changes in FRET we needed to rely on two assumptions: first, FRET experiments revealed that the maximal ratiometric FRET signal of single living HUVECs was stable after equilibration with external buffer; thus, we assumed that [cAMP] is less than 10 nM at resting conditions (R_0) according to the *in vitro* calibration of Epac1-camps. Second, the ratiometric FRET signal reached a stable minimum with kinetics indicative of sensor saturation upon stimulation of cells with 1 μM isoproterenol. Therefore, we concluded that cAMP levels were elevated to more than 100 μM (R_{iso}) at maximal concentrations of the isoproterenol. Analysis of FRET experiments with a stable minimum of the ratiometric FRET signal after stimulation of HUVECs with 1 μM isoproterenol (representative experiment shown in Fig. 3*E* right) revealed a mean $R_{iso} - R_0$ value of -0.55 ± 0.01 ($n = 16$). Thus, we established an *in vivo* calibration curve for Epac1-camps reaching from 0 to −0.55. Based on this *in vivo* calibration, we calculated cAMP levels of control or transfected cells after stimulation with 10 nM isoprenaline, and the respective thrombin-mediated changes in [cAMP] (Fig. 3*F*). In control cells, [cAMP] rose to 1.2 ± 0.2 μM and was decreased by 0.4 ± 0.1 μM ($n = 17$) after thrombin treatment. In AC6-overexpressing cells, [cAMP] increased to 1.7 ± 0.2 μM and was diminished by 1.1 ± 0.2 μM ($n = 17$), whereas in AC4-overexpressing cells the rise in [cAMP] to 0.4 ± 0.1 μM was further increased by 0.4 ± 0.1 μM ($n = 15$) 30 s after thrombin application. The respective thrombin-induced changes in [cAMP] of AC6- and AC4-overexpressing cells were significantly different compared to control cells ($P < 0.01$, Fig. 3*F*). The clear dependency of the thrombin-induced changes in cAMP levels on the expressed AC subtype pointed towards the hypothesis that the Ca^{2+}-dependent decrease in [cAMP] was due to inhibition of endogenous AC activity.

Downregulation of AC5 and AC6 by siRNA abolishes the thrombin-mediated decrease in [cAMP]

To directly test the involvement of AC5 and AC6 in the Ca^{2+}-mediated decrease in [cAMP], we downregulated the respective adenylyl cyclases using specific siRNA pools. HUVECs were transfected with either a non-targeting siRNA pool as a negative control or with AC5 and AC6 siRNA pools (see Methods). For the quantitative analysis of AC5 and AC6 mRNA after siRNA transfections, we performed real-time PCR for AC5 mRNA and AC6 mRNA, respectively, using GAPDH mRNA as internal reference. AC6 mRNA was significantly reduced ($n = 3$; $P < 0.01$) in HUVECs that were transfected with AC5/6 siRNA relative to control cells that were transfected with non-targeting siRNA, as revealed by $2^{-\Delta\Delta CT}$ analysis of real-time PCR data (Fig. 4*A*). However, the overall amount of AC5 mRNA was too low (<0.05% of AC6 mRNA; data not shown) to detect a siRNA-mediated downregulation. This is in agreement with real-time PCR data of Bundey & Insel (2003) that detected only minor amounts of AC5 transcripts in HUVECs compared to AC6 transcripts.

A representative FRET trace of HUVECs that were transfected with non-targeting siRNA shows that the thrombin-mediated increase in FRET was not affected by siRNA transfection (Fig. 4*B*). However, transfection of AC5/6 siRNA resulted in a complete loss of the thrombin-induced increase in FRET and revealed a thrombin-mediated decrease in FRET instead (representative FRET trace, Fig. 4*C*). Additionally, downregulation of AC6 mRNA resulted in a significantly diminished isoproterenol-induced decrease of ratiometric FRET signals ($R_{iso} - R_0$) after stimulation of HUVECs with 10 nM isoproterenol ($P < 0.01$). However, this effect could be compensated by stimulation of AC5/6 siRNA-transfected cells with 30 nM isoproterenol (Fig. 4*D*). The addition of thrombin to prestimulated HUVECs led to a further decrease in FRET. Thus, examination of $R_{thrombin}$ values 30 s after thrombin application revealed negative values of $R_{thrombin} - R_{iso}$ (Fig. 4*E*). This thrombin-mediated decrease of ratiometric FRET signals ($R_{thrombin} - R_{iso}$) in AC5/6 siRNA-transfected HUVECs was also seen in cells that were prestimulated with 30 nM isoproterenol, which led to elevation of cAMP levels comparable to control cells (Fig. 4*E*). Thus, downregulation of the predominant subtype AC6 abolished the thrombin-mediated decrease

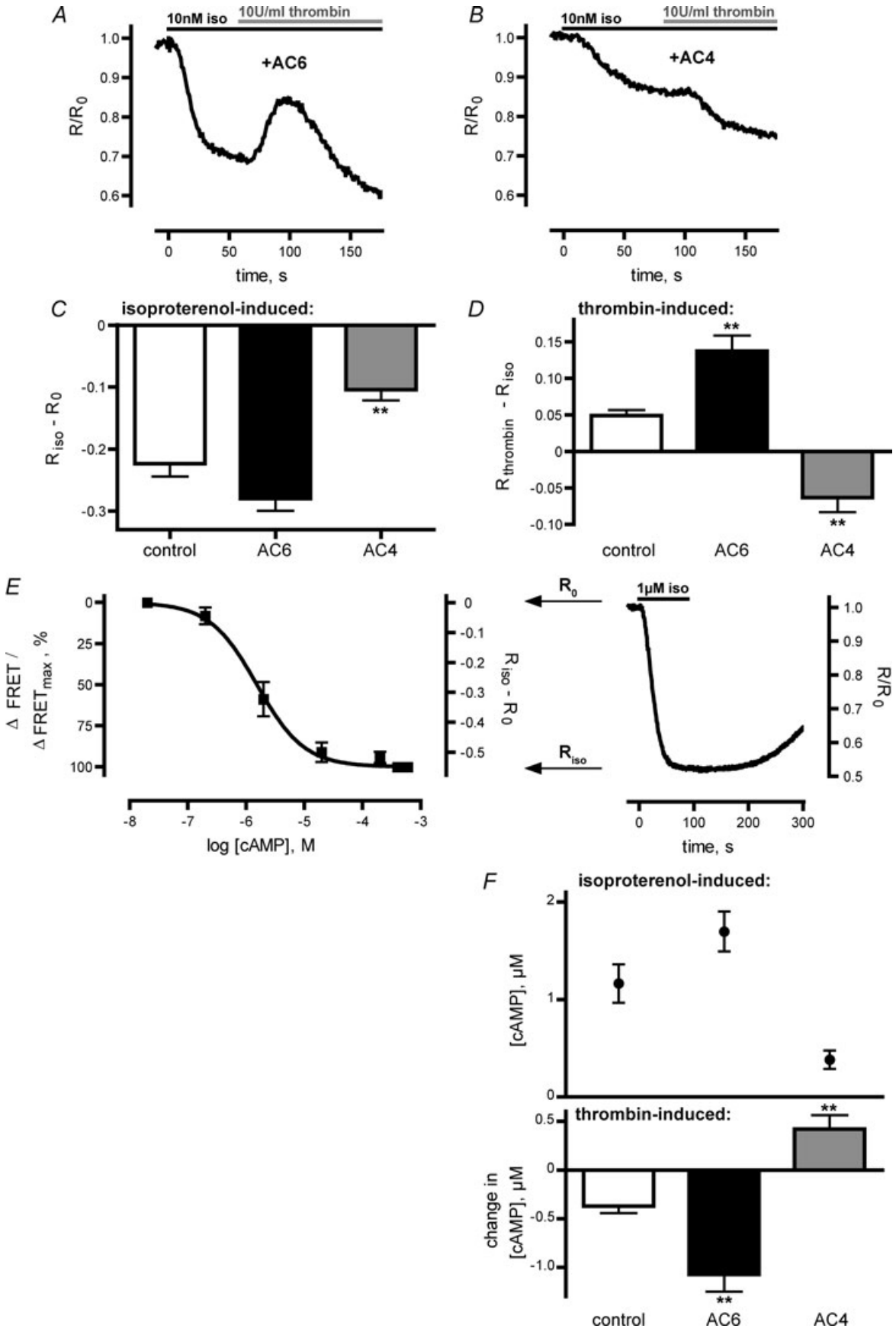

in [cAMP] and uncovered a thrombin-mediated increase in [cAMP].

Using the calibration curve of Epac1-camps (Fig. 3*E*) we calculated [cAMP] after stimulation with isoproterenol and subsequent changes in [cAMP] after addition of thrombin (Fig. 4*F*). In control cells, transfected with non-targeting siRNA, [cAMP] increased to $1.0 \pm 0.1\ \mu$M ($n = 22$) after isoproterenol stimulation (10 nM). Thrombin treatment led to a reduction of cAMP levels by $0.3 \pm 0.1\ \mu$M. In AC5/6 siRNA-transfected cells, cAMP levels rose to $0.5 \pm 0.1\ \mu$M ($n = 23$) and $1.0 \pm 0.3\ \mu$M ($n = 12$) after stimulation with 10 nM and 30 nM isoproterenol, respectively. Thrombin application led to a further increase in [cAMP] by $0.3 \pm 0.1\ \mu$M (10 nM isoproterenol) and $0.4 \pm 0.1\ \mu$M (30 nM isoproterenol, Fig. 4*F*) and these changes in [cAMP] were significantly different when compared to those of control cells ($P < 0.01$).

In summary, we observed a transient thrombin-mediated decrease of pre-elevated cAMP levels in HUVECs and demonstrated that this effect is not due to G_i protein activation, but rather is dependent on a Ca^{2+}-mediated inhibition of AC6.

Discussion

Ca^{2+} and cAMP signals control the barrier function of endothelial cells. While a rise in intracellular Ca^{2+} enhances permeability of endothelial cells, a local increase in [cAMP] at the cell membrane is barrier protective via an increased adhesion of the cells. Thrombin is discussed to increase endothelial permeability due to a Ca^{2+}-mediated endothelial cell contraction, but also by decreasing barrier protective cAMP levels (Mehta & Malik, 2006; Michel & Curry, 1999). The crosstalk regulation between Ca^{2+} and cAMP signals may play an important role for a fine-tuned barrier function. Therefore, we studied the impact of thrombin-induced Ca^{2+} signals on elevated cAMP levels with high temporal resolution. By using the Ca^{2+}-sensitive dye Fluo-4 and the FRET-based cAMP sensor Epac1-camps we monitored Ca^{2+} and cAMP signals in real time in living HUVECs. Epac1-camps-transfected HUVECs were prestimulated with isoproterenol to elevate cAMP levels to $1.2 \pm 0.2\ \mu$M. Additional stimulation with thrombin evoked a decrease of cAMP levels of $0.4 \pm 0.1\ \mu$M (Fig. 3*F*). This is similar to data obtained by standard radioimmunoassay techniques where a Ca^{2+}-mediated decrease of basal and elevated cAMP levels by 20–50% was detected in pulmonary artery endothelial cells (PAECs) and pulmonary microvascular endothelial cells (PMVECs; Stevens *et al.* 1995; Cioffi *et al*. 2002). However, due to the high temporal resolution of FRET-based assays, we found this decrease in [cAMP] to be transient (see below) with minimal cAMP levels 30 s after thrombin application and cAMP levels to recover within 1.5 min (Fig. 1*C*). Other studies that examined endothelial permeability demonstrated a thrombin-enhanced permeability within 0.5 min as detected by a decrease in electrical impedance of monolayers of bovine PAECs and PMVECs (Tiruppathi *et al.* 1992). Similarly, a maximum transendothelial albumin clearance rate occurred within 2 min in confluent bovine PAECs (Lum *et al.* 1992). These results imply a fast Ca^{2+}-mediated regulation of cAMP signals, as detected in the present study. However, this thrombin-evoked increase in permeability is described to last for up to 2 h (Tiruppathi *et al.* 1992), whereas cAMP levels were only transiently decreased in the present study. The fast and transient decrease in [cAMP] only explains an initial increase in permeability. One possible explanation for this inconsistency is that thrombin- or histamine-induced increases in endothelial permeability were only detected in cells that were not prestimulated with forskolin or isoproterenol, whereas, for example, a histamine-induced increase in permeability in HUVECs was prevented when cells were pretreated with forskolin (Carson *et al.* 1989). So possibly the transient decrease in [cAMP] detected in this study might not be sufficient to

Figure 3. Overexpression of AC4 and AC6 influenced the thrombin-induced decrease of cAMP levels
A, representative FRET trace of AC6-transfected HUVECs demonstrates that overexpression of AC6 enhanced the increase in FRET. *B*, overexpression of AC4 abolished the transient increase in FRET, revealing a thrombin-induced decrease in FRET (representative experiment). *C*, overexpression of AC6 and AC4 influenced the amount of decrease in ratiometric FRET ($R_{iso} - R_0$) following stimulation with 10 nM isoproterenol. Overexpression of AC6 enhanced G_s-mediated decrease of $R_{iso} - R_0$, whereas overexpression of AC4 reduced isoproterenol-induced decrease of $R_{iso} - R_0$. *D*, the thrombin-mediated increase of ratiometric FRET signals ($R_{thrombin} - R_{iso}$) was enhanced in HUVECs overexpressing AC6 and reduced in cells overexpressing AC4. *E*, to estimate changes in [cAMP] in living cells we measured an *in vitro* concentration–response curve for Epac1-camps (left). Assuming [cAMP] < 10 nM under resting conditions (R_0) and sensor saturation at [cAMP] > 100 μM after stimulation of cells with 1 μM isoproterenol (R_{iso}), we established a concentration–response curve with ΔFRET values ranging from 0 (R_0) to −0.55, that is representing the mean of 16 values of $R_{iso} - R_0$ after stimulation with 1 μM isoproterenol (representative experiment shown, right). *F*, with help of the calibration curve of Epac1-camps (*E*), changes in ratiometric FRET were translated into [cAMP]. We determined [cAMP] in control cells and in AC6- or AC4-transfected cells after stimulation with 10 nM isoproterenol (above) and the respective change in [cAMP] after thrombin treatment (bottom). $^{**}P < 0.01$.

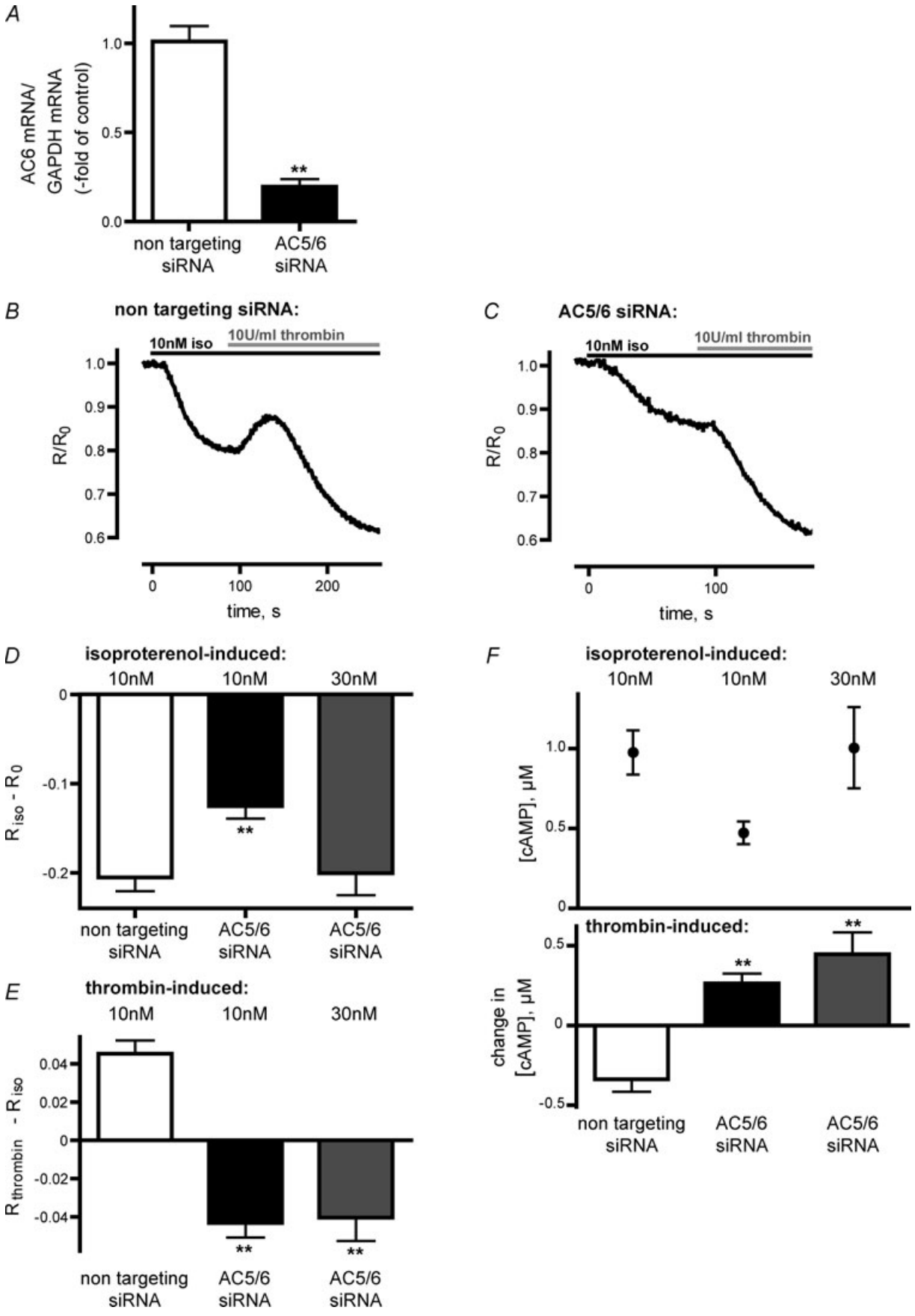

induce a sustained increase in permeability. Additionally one has to keep in mind that in this study we measured global cAMP levels, but cAMP compartmentation might be relevant for barrier regulation and cytoplasmic cAMP was demonstrated to increase endothelial permeability (Sayner *et al.* 2006). The measurement of locally defined cAMP pools remains an ambitious task for future studies.

We estimated [cAMP] and thrombin-induced changes in [cAMP] in intact cells by comparison with *in vitro*-calibrated FRET signals (Fig. 3*E*). A reliable estimation of *in vivo* cAMP levels was based on the two assumptions that the cAMP level of single HUVECs is less than 10 nM after equilibration with external buffer and that [cAMP] was elevated to more than 100 μM at maximal concentrations of isoproterenol. By using the *in vitro* calibration of Epac1-camps we claim to obtain rather approximate values for [cAMP] in intact cells.

The thrombin receptor PAR-1 is described to interact with G_q, $G_{12/13}$ and with the PTX-sensitive G_i protein (McLaughlin *et al.* 2005; Ayoub *et al.* 2007; Vandenbroucke *et al.* 2008). A thrombin-induced decrease of elevated cAMP levels in rat adrenal medullary microvascular endothelial cells was demonstrated to be due to a G_i-mediated inhibition of adenylyl cyclases (Manolopoulos *et al.* 1997). However, our experiments revealed that the thrombin-mediated decrease in [cAMP] in HUVECs was not caused by the activation of G_i protein as incubation of cells with PTX did not significantly affect the decrease of cAMP levels (Fig. 2*B*). Therefore, we focused on the Ca^{2+}-mediated regulation of cAMP signals. The examination of thrombin-induced Ca^{2+} signals in Fluo-4-labelled HUVECs revealed a rapid increase in $[Ca^{2+}]_i$ that peaked approximately 15 s after thrombin application and a slow decrease in $[Ca^{2+}]_i$ lasting over 200 s (Fig. 1*B*) comparable to Ca^{2+} measurements in Fura-2-loaded bovine PAECs (Lum *et al.* 1992). The long-lasting Ca^{2+} signal may reflect capacitative Ca^{2+} entry that is provoked by Ca^{2+} release from intracellular stores. Removal of Ca^{2+} from an EGTA-buffered external solution during FRET experiments significantly reduced the thrombin-induced decrease of elevated cAMP levels (Fig. 2*B*). We concluded, therefore, that the decrease of cAMP levels is Ca^{2+}-dependent. As endothelial cells do express Ca^{2+}-inhibited AC5 and AC6 (Manolopoulos *et al.* 1995; Stevens *et al.* 1995; Chetham *et al.* 1997; Bundey & Insel, 2003) and capacitative Ca^{2+} entry is discussed to be a potent regulator of AC5 and AC6 (Chiono *et al.* 1995; Fagan *et al.* 1998), we investigated the Ca^{2+}-mediated inhibition of AC5 and AC6.

The thrombin-induced decrease in [cAMP] was completely abolished in HUVECs that were transfected with siRNA against AC5 and AC6 (Fig. 4*F*). AC6 was found to be the predominant Ca^{2+}-inhibited subtype in HUVECs (compare Bundey & Insel, 2003) and we demonstrate for the first time directly that the thrombin-mediated decrease in [cAMP] is due to the Ca^{2+}-mediated inhibition of AC6. These data suggest that the Ca^{2+}-mediated inhibition of AC6 is the primary mechanism by which thrombin induces a transient decrease in cAMP subsequent to adrenoceptor-mediated stimulation.

We could exclude a significant involvement of the Ca^{2+}-activated PDE1 and suggested that PDE1 is not functionally expressed in HUVECs, as we could not detect any effect of the PDE1-selective inhibitor 8MM-IBMX that is seen in PDE1-expressing cells. This was already reported from other studies where no significant PDE1 activity was detectable in HUVECs (Netherton & Maurice, 2004; Seybold *et al.* 2005). A possible minor contribution from PDE2 indirectly activated via Ca^{2+}, NO production and subsequent cGMP generation cannot be excluded (Surapisitchat *et al.* 2007).

Our data further support the hypothesis that the Ca^{2+}-mediated inhibition of AC6 may be essential for a thrombin-mediated endothelial cell gap formation as reported by Cioffi *et al.* (2002). This group showed that overexpression of the Ca^{2+}-stimulated AC8 in PAECs and PMVECs abolished a thrombin-induced increase in permeability. We assume that the Ca^{2+}-mediated inhibition of pre-activated AC6 might be a mechanism

Figure 4. Downregulation of AC5 and AC6 by siRNA resulted in abolishment of the thrombin-mediated decrease in [cAMP]

A, AC6 transcripts of HUVECs, that were transfected with non-targeting siRNA or AC5/6 siRNA, were analysed by real-time quantitative PCR and normalised to GAPDH transcripts. Analysis of real-time data revealed a reduction of AC6 transcripts in AC5/6 siRNA-transfected HUVECs relative to control cells, transfected with non-targeting siRNA ($n = 3$). *B*, a representative FRET trace of HUVECs, transfected with non-targeting siRNA and Epac1-camps, depicts a transient increase in FRET followed by a decrease in FRET. *C*, a representative FRET trace of HUVECs, transfected with AC5/6 siRNA and Epac1-camps, demonstrates that downregulation of AC5/6 abolished the transient increase in FRET and resulted in a decrease in FRET. *D*, transfection of HUVECs with AC5/6 siRNA resulted in a diminished decrease of ratiometric FRET signals ($R_{iso} - R_0$) following stimulation of cells with 10 nM isoproterenol compared to control cells. This effect was compensated by stimulation of cells with 30 nM isoproterenol. *E*, thrombin application resulted in a decrease of ratiometric FRET signals ($R_{thrombin} - R_{iso}$) in HUVECs transfected with AC5/6 siRNA in contrast to control cells transfected with non-targeting siRNA. *F*, [cAMP] and changes in [cAMP] were calculated from the respective isoproterenol- (*D*) and thrombin-induced FRET changes (*E*) by using the [cAMP] calibration curve of Epac1-camps (Fig. 3*E*). $^{**}P < 0.01$.

to induce endothelial cell gap formation despite receptor-mediated pre-elevation in [cAMP]. As in the absence of agonist we could not observe a basal increase in [cAMP] even if AC6 was overexpressed, we conclude that receptor-independent activity of AC6 is rather low and therefore Ca^{2+}-mediated inhibition of AC6 may affect cAMP levels only when G_s-coupled receptors are activated.

As mentioned above, we unexpectedly observed a transient decrease of cAMP levels with the levels recovering within about 1.5 min after thrombin application. This transient decrease of cAMP levels is not consistent with results of radioimmuno-based cAMP assays. In these assays, a decrease of cAMP levels was detected after a 5 min incubation of cells (PAECs and PMVECs) with thrombin in the presence of PDE inhibitors (Stevens *et al.* 1995; Cioffi *et al.* 2002). However, one cannot directly compare results of enzyme-/radio-immuno-based and FRET-based cAMP assays. Enzyme- and radio-immuno-based assays measure total [cAMP] of cell lysates relative to protein content or cell number. It is difficult to determine the exact cytosolic volume and therefore the absolute concentration of cAMP with these conventional assays. Therefore, it is particularly difficult to accurately measure small changes in [cAMP] with high temporal resolution. In contrast, FRET-based assays allow the estimation of absolute [cAMP] of single living cells within cell monolayers and the detection of exact time frames of Ca^{2+}-mediated changes in [cAMP] due to real-time measurement and a rapid superfusion system for the controlled application of agonists. The transient decrease of cAMP levels could reflect the transient increase in Ca^{2+} signals, but there was a long-lasting plateau phase and AC5 and AC6 are discussed to be potently inhibited by capacitative Ca^{2+} entry (Fagan *et al.* 1998). Alternatively, the transient decrease of cAMP levels could reflect a subsequent thrombin-mediated increase of cAMP levels that we observed when HUVECs were not prestimulated with isoproterenol to elevate cAMP levels (Fig. 1*D*) and was also uncovered in cells that were transfected with Ca^{2+}-independent AC4 (Fig. 3*B*) or in cells where AC5 and AC6 were down-regulated (Fig. 4*C*). The overexpression of AC4 also seemed to compete with endogenous AC5 and AC6 as a thrombin-mediated decrease in [cAMP] could not be detected. The mechanism leading to a thrombin-mediated increase of cAMP levels is the topic of ongoing studies. A thrombin-induced transient decrease in basal [cAMP] cannot be excluded due to the binding affinity of the sensor. However, most of the cAMP-regulated proteins require [cAMP] above 100 nM. Therefore, such a potential decrease in [cAMP] is not expected to regulate cellular function.

Furthermore, our FRET data of HUVECs transfected with siRNA against AC5 and AC6 (Fig. 4*D*) suggest that AC6 represents the functionally predominant AC subtype in HUVECs, as cAMP levels evoked by stimulation with isoproterenol were significantly reduced in these cells.

In summary, our study presented for the first time a real-time monitoring of thrombin-induced changes in [cAMP] in living endothelial cells. Using a FRET-based cAMP sensor we observed a transient decrease of elevated cAMP levels upon thrombin application in HUVECs. Downregulation of the predominant subtype AC6 in HUVECs provided the first direct evidence that the Ca^{2+}-mediated inhibition of AC6 in HUVECs is responsible for the thrombin-mediated decrease of cAMP levels.

References

Ayoub MA, Maurel D, Binet V, Fink M, Prezeau L, Ansanay H & Pin JP (2007). Real-time analysis of agonist-induced activation of protease-activated receptor 1/Gai1 protein complex measured by bioluminescence resonance energy transfer in living cells. *Mol Pharmacol* **71**, 1329–1340.

Barr AJ, Brass LF, Manning DR (1997). Reconstitution of receptors and GTP-binding regulatory proteins (G proteins) in Sf9 cells. A direct evaluation of selectivity in receptor.G protein coupling. *J Biol Chem.* **272**, 2223–2229.

Bogatcheva NV, Garcia JG & Verin AD (2002). Molecular mechanisms of thrombin-induced endothelial cell permeability. *Biochemistry (Mosc)* **67**, 75–84.

Bundey RA & Insel PA (2003). Quantification of adenylyl cyclase messenger RNA by real-time polymerase chain reaction. *Anal Biochem.* **319**, 318–322.

Carson MR, Shasby SS & Shasby DM (1989). Histamine and inositol phosphate accumulation in endothelium: cAMP and a G protein. *Am J Physiol Lung Cell Mol Physiol* **257**, L259–L264.

Chetham PM, Guldemeester HA, Mons N, Brough GH, Bridges JP, Thompson WJ & Stevens T (1997). Ca^{2+}-inhibitable adenylyl cyclase and pulmonary microvascular permeability. *Am J Physiol Lung Cell Mol Physiol* **273**, L22–L30.

Chiono M, Mahey R, Tate G & Cooper DM (1995). Capacitative Ca^{2+} entry exclusively inhibits cAMP synthesis in C6-2B glioma cells. Evidence that physiologically evoked Ca^{2+} entry regulates Ca^{2+}-inhibitable adenylyl cyclase in non-excitable cells. *J Biol Chem* **270**, 1149–1155.

Cioffi DL, Moore TM, Schaack J, Creighton JR, Cooper DM & Stevens T (2002). Dominant regulation of interendothelial cell gap formation by calcium-inhibited type 6 adenylyl cyclase. *J Cell Biol* **157**, 1267–1278.

Creighton JR, Masada N, Cooper DM & Stevens T (2003). Coordinate regulation of membrane cAMP by Ca2+-inhibited adenylyl cyclase and phosphodiesterase activities. *Am J Physiol Lung Cell Mol Physiol* **284**, L100–L107.

Fagan KA, Mons N & Cooper DM (1998). Dependence of the Ca^{2+}-inhibitable adenylyl cyclase of C6-2B glioma cells on capacitative Ca^{2+} entry. *J Biol Chem* **273**, 9297–9305.

Garcia JG, Davis HW & Patterson CE (1995). Regulation of endothelial cell gap formation and barrier dysfunction: role of myosin light chain phosphorylation. *J Cell Physiol* **163**, 510–522.

Goraya TA & Cooper DM (2005). Ca^{2+}-calmodulin-dependent phosphodiesterase (PDE1): current perspectives. *Cell Signal* **17**, 789–797.

Hein P, Rochais F, Hoffmann C, Dorsch S, Nikolaev VO, Engelhardt S, Berlot CH, Lohse MJ & Bünemann M (2006). Gs activation is time-limiting in initiating receptor-mediated signaling. *J Biol Chem* **281**, 33345–33351.

Livak KJ & Schmittgen TD (2001). Analysis of relative gene expression data using real-time quantitative PCR and the $2^{-\mathrm{DD}CT}$ method. *Methods* **25**, 402–408.

Lum H, Aschner JL, Phillips PG, Fletcher PW & Malik AB (1992). Time course of thrombin-induced increase in endothelial permeability: relationship to $Ca^{2+}{}_i$ and inositol polyphosphates. *Am J Physiol Lung Cell Mol Physiol* **263**, L219–L225.

Lum H, Del Vecchio PJ, Schneider AS, Goligorsky MS & Malik AB (1989). Calcium dependence of the thrombin-induced increase in endothelial albumin permeability. *J Appl Physiol.* **66**, 1471–1476.

McLaughlin JN, Shen L, Holinstat M, Brooks JD, DiBenedetto E & Hamm HE (2005). Functional selectivity of G protein signaling by agonist peptides and thrombin for the protease-activated receptor-1. *J Biol Chem* **280**, 25048–25059.

Manolopoulos VG, Fenton JW 2nd & Lelkes PI (1997). The thrombin receptor in adrenal medullary microvascular endothelial cells is negatively coupled to adenylyl cyclase through a Gi protein. *Biochim Biophys Acta* **1356**, 321–332.

Manolopoulos VG, Liu J, Unsworth BR & Lelkes PI (1995). Adenylyl cyclase isoforms are differentially expressed in primary cultures of endothelial cells and whole tissue homogenates from various rat tissues. *Biochem Biophys Res Commun* **208**, 323–331.

Mehta D & Malik AB (2006). Signaling mechanisms regulating endothelial permeability. *Physiol Rev* **86**, 279–367.

Michel CC & Curry FE (1999). Microvascular permeability. *Physiol Rev* **79**, 703–761.

Minnear FL, DeMichele MA, Moon DG, Rieder CL & Fenton JW 2nd (1989). Isoproterenol reduces thrombin-induced pulmonary endothelial permeability in vitro. *Am J Physiol Heart Circ Physiol* **257**, H1613–H1623.

Mou TC, Masada N, Cooper DMF & Sprang SR (2009). Structural basis for inhibition of mammalian adenylyl cyclase by calcium. *Biochemistry* **48**, 3387–3397.

Netherton SJ & Maurice DH (2004). Vascular endothelial cell cyclic nucleotide phosphodiesterases and regulated cell migration: implications in angiogenesis. *Mol Pharmacol* **67**, 263–272.

Nikolaev VO, Bünemann M, Hein L, Hannawacker A & Lohse MJ (2004). Novel single chain cAMP sensors for receptor-induced signal propagation. *J Biol Chem* **297**, 37215–37218.

Putney JW Jr & Bird GS (1993). The signal for capacitative calcium entry. *Cell* **75**, 199–201.

Sadana R & Dessauer CW (2009). Physiological roles for G protein-regulated adenylyl cyclase isoforms: insights from knockout and overexpression studies. *Neurosignals* **17**, 5–22.

Sayner SL, Alexeyev M, Dessauer CW & Stevens T (2006). Soluble adenylyl cyclase reveals the significance of cAMP compartmentation on pulmonary microvascular endothelial cell barrier. *Circ Res* **98**, 675–681.

Seybold J, Thomas D, Witzenrath M, Boral S, Hocke AC, Bürger A, Hatzelmann A, Tenor H, Schudt C, Krüll M, Schütte H, Hippenstiel S & Suttorp N (2005). Tumor necrosis factor-α-dependent expression of phosphodiesterase 2: role in endothelial hyperpermeability. *Blood* **105**, 3569–3576.

Stelzner TJ, Weil JV & O'Brien RF (1989). Role of cyclic adenosine monophosphate in the induction of endothelial barrier properties. *J Cell Physiol* **139**, 157–166.

Stevens T, Creighton J & Thompson WJ (1999). Control of cAMP in lung endothelial cell phenotypes. Implications for control of barrier function. *Am J Physiol Lung Cell Mol Physiol* **277**, L119–L126.

Stevens T, Nakahashi Y, Cornfield DN, McMurtry IF, Cooper DM & Rodman DM (1995). Ca^{2+}-inhibitable adenylyl cyclase modulates pulmonary artery endothelial cell cAMP content and barrier function. *Proc Natl Acad Sci U S A* **92**, 2696–2700.

Surapisitchat J, Jeon KI, Yan C & Beavo JA (2007). Differential regulation of endothelial cell permeability by cGMP via phosphodiesterases 2 and 3. *Circ Res* **101**, 811–818.

Tiruppathi C, Malik AB, Del Vecchio PJ, Keese CR & Giaever I (1992). Electrical method for detection of endothelial cell shape change in real time: assessment of endothelial barrier function. *Proc Natl Acad Sci U S A* **89**, 7919–7923.

Vandenbroucke E, Mehta D, Minshall R & Malik AB (2008). Regulation of endothelial junctional permeability. *Ann N Y Acad Sci* **1123**, 134–145.

Willoughby D & Cooper DM (2007). Organization and Ca^{2+} regulation of adenylyl cyclases in cAMP microdomains. *Physiol Rev* **87**, 965–1010.

Wysolmerski RB & Lagunoff D (1990). Involvement of myosin light-chain kinase in endothelial cell retraction. *Proc Natl Acad Sci U S A* **87**, 16–20.

Author contributions

Ruth C. Werthmann performed the majority of experiments, their analyses and wrote the manuscript. Kathrin von Hayn conducted specific experiments. Viacheslav O. Nikolaev helped to design specific experiments. Martin J. Lohse significantly contributed to the study design and writing of the manuscript. Moritz Bünemann conceived the experiments and wrote the manuscript. All parts of this study were conducted at the Department of Pharmacology and Toxicology, University of Würzburg, except real-time PCR that was performed at the Department of Internal Medicine I, University of Würzburg.

Acknowledgements

We are grateful to Annette Hannawacker for technical assistance during the *in vitro* calibration of Epac1-camps, Alexander Zürn for confocal images of VE-cadherin staining and Leif Hommers for critically reading the manuscript (Department of Pharmacology and Toxicology, University of Würzburg). We thank Jan Fiedler and Dr Thomas Thum (Department

of Internal Medicine I, University of Würzburg) for the technical support to perform real-time PCR experiments. Plasmids encoding AC4 and AC6 were kindly supplied by Professor Dermot MF Cooper (Department of Pharmacology, University of Cambridge, UK). We thank Professor Jens Waschke for kindly providing VE-cadherin antibodies. This work was supported by the Deutsche Forschungsgemeinschaft (SFB 688, TP B6).